

# Impact of land use/land cover change on regional hydrometeorology in Amazonia

Somnath Baidya Roy

Department of Ecology and Evolutionary Biology, Princeton University, Princeton, New Jersey, USA

Roni Avissar

Department of Civil and Environmental Engineering, Duke University, Durham, North Carolina, USA

Received 15 December 2000; revised 7 June 2001; accepted 12 June 2001; published 22 August 2002

[1] A high-resolution mesoscale model was used to investigate the impact of deforestation in Amazonia. Coherent mesoscale circulations were triggered by the surface heterogeneity; synoptic flow did not eliminate the circulations but advected them away from the location where they were generated. This was substantiated by satellite-derived cloud images. These circulations affected the transport of moisture and heat at the synoptic scale and can affect climate. Adequate parameterizations for these processes should be included in GCMs for more accurate climate simulations.

INDEX TERMS: 3322

Meteorology and Atmospheric Dynamics: Land/atmosphere interactions; 3307 Meteorology and Atmospheric Dynamics: Boundary layer processes; 3314 Meteorology and Atmospheric Dynamics: Convective processes; 1833 Hydrology: Hydroclimatology; 3329 Meteorology and Atmospheric Dynamics: Mesoscale meteorology

KEYWORDS: Amazonia, surface heterogeneity, mesoscale flow, RAMS, shallow cumulus, heat flux.

## 1. Introduction

[2] Differential heating of the planetary boundary layer (PBL) due to heterogeneity in the underlying Earth surface gives rise to atmospheric circulations over a wide range of spatial and temporal scales. At the mesoscale, sea breeze and lake breeze produced by the thermal gradient between adjacent land and water bodies are interesting examples of this type of circulation. Significant natural and human-induced heterogeneity, existing within the land surface in the form of patches, whose radiative and thermal properties differ from those of their surroundings, can also produce horizontal temperature and pressure gradients strong enough to generate and sustain organized mesoscale circulations of a similar nature [Segal and Arritt, 1992].

[3] The resolution of conventional meteorological observational networks is too coarse to capture these circulations. However, a few dedicated field experiments have indicated that such mesoscale circulations can indeed be produced by naturally occurring surface flux contrasts [Physick and Tapper, 1990; Segal et al., 1991].

[4] Large-scale agriculture and deforestation can contribute significantly to the patchiness of the existing landscape. Only a few studies have used observational data to look into the impact of human activities. They have found that despite strong thermal contrasts between perturbed and nonperturbed areas, the resulting circulations are shallow and weak and often damped by strong large-scale gradients [Doran et al., 1995; Mahrt et al., 1994; Segal et al., 1989]. Satellite images however, provide evidence for the existence of organized circulations strong enough to produce cumulus clouds [Rabin et al., 1990; Cutrim et al., 1995; Rabin and Martin, 1996; Weaver and Avissar, 2001].

[5] Analytical and numerical studies have shown that heterogeneity in surface sensible and latent heat flux can produce strong mesoscale circulations [Avissar and Liu, 1996; Avissar and Schmidt, 1998; Wang et al., 1996, 1998]. These circulations significantly affect the structure of the PBL, fluxes of heat, moisture and scalars [Chen and Avissar, 1994a; Dalu and Pielke, 1993; Dalu et al., 1996; Li and Avissar, 1994; Lynn et al., 1995], and organization of clouds and precipitation [Chen and Avissar, 1994b; Wang et al., 2000; Wetzel et al., 1996].

[6] Most of these earlier simulations used idealized patterns of surface heterogeneity and neglected the interaction of the mesoscale with synoptic-scale processes. Some found that even a moderate background wind is capable of nearly eliminating the mesoscale circulations [Avissar and Schmidt, 1998]. Recent studies, using sophisticated models and incorporating realistic synoptic-scale conditions have reported the evolution of coherent mesoscale circulations in response to surface heat flux patchiness [Dolman et al., 1999; Seth and Giorgi, 1996; Vidale et al., 1997]. Wang et al. [2000] found that surface-driven mesoscale circulations can trigger moist convection leading to clouds and precipitation under weak stability and synoptic wind conditions. However, using a broad range of observed synoptic-scale conditions in the central United States, Weaver and Avissar [2001] have shown that strong large-scale winds do not necessarily inhibit the mesoscale circulations. Their conclusions were supported by a wide array of observations, including satellite images, radars, and an extensive network of rain gauges.

[7] The exchange of energy, moisture, and momentum between the land surface and the atmosphere is an important component of the climate system. By affecting these fluxes, mesoscale circulations can potentially affect atmospheric circulations at the global scale [Copeland et al., 1996; Pielke et al., 1998]. In contrast, Zhong and Doran [1997, 1998] have argued that the impacts are strictly local.

[8] In the work presented in this paper, a state-of-the-art

mesoscale model was used to simulate the impact of land-surface heterogeneity caused by deforestation in Amazonia under realistic environmental conditions. Large-scale deforestation of the Amazonian rain forest began in the 1970s and continued unabated till the early 1990s [Fearnside, 1993; Skole and Tucker, 1993]. The pattern of deforestation is quite unique, following the expanding road network, creating the well-known “fish-bone” structure. The rate of deforestation has slowed down since then due to a variety of reasons, and now it seems unlikely that the entire rain forest will be wiped out. A significant part of the climatological and hydrological effects of this deforestation will probably be through the mesoscale circulations generated by the heterogeneous land surface [Dolman *et al.*, 1999; Gash and Nobre, 1997]. The study by Cutrim *et al.* [1995], showing increasing cloudiness over deforested patches, is a “footprint” of this phenomenon.

[9] Here satellite data have been used to validate the results of our simulations. Weaver and Avissar [2001] successfully used a similar approach to investigate the effects of agriculture in the central United States. By demonstrating that mesoscale circulations generated by landscape heterogeneity can be produced in different climatological regions under various meteorological conditions, we intend to prove that such circulations are important components of the climate system. Therefore the present study, which focuses on the tropical region, is another step toward this objective.

[10] In section 2 the details of the numerical experiment are discussed. Section 3 contains the results of the simulations and comparison with satellite data. Finally, the implications of this study are discussed in section 4.

## 2. Numerical Experiment

### 2.1. Study Area

[11] The study area was located in the state of Rondônia in northwestern Brazil. Rondônia forms the southwestern boundary of the “legal Amazon,” a 5 million km<sup>2</sup> administrative area covering six states in full and parts of three states. In the 1980s, 10–20% of forest in this state was lost due to systematic encroachment by humans. In the previous decade, compelled by a host of domestic and international factors, Brazilian agriculture went through rapid changes, including increased mechanization and shift toward export-oriented but less labor-intensive crops such as soybean and wheat. This resulted in a large surplus of farm labor. To solve the issue of these landless farmers, as well as that of overpopulation in the coastal states, the Brazilian government started a program of aggressive colonization of Amazonia, which was then seen as an untamed frontier ready for economic exploitation. Settlers were given small 2-acre plots for farming and ranching along the rapidly expanding network of highways (like BR-364) and local roads, leading to the well-known “fishbone” structure, the dominant pattern of deforestation in Rondônia [Fearnside, 1993; Skole and Tucker, 1993; Skole *et al.*, 1994].

[12] The complexity of the landscape heterogeneity in Rondônia (described in detail by Calvet *et al.*, [1997] showing fine structures, only a few kilometers in width, embedded within ~100 km wide swaths), combined with the relatively sharp gradient between the forested and the deforested patches, makes this region ideal for development of coherent mesoscale circulations.

### 2.2. Model Description and Setup

[13] The Regional Atmospheric Modeling System (RAMS) [Pielke *et al.*, 1992; Liston and Pielke, 2000] was used for our

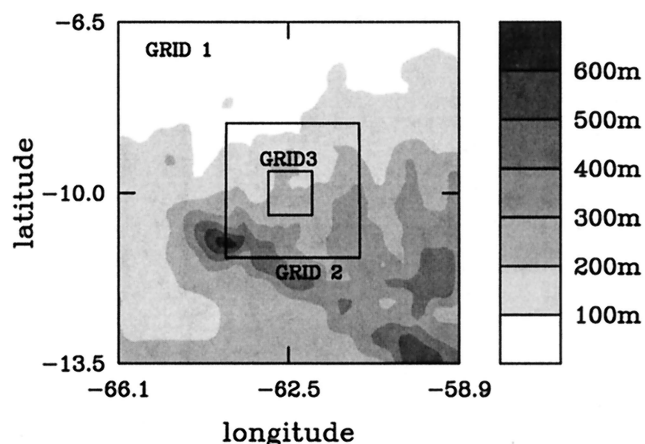


**Figure 1.** Study area showing the three nested grids and orography.

simulations. RAMS solves all the three-dimensional, compressible, nonhydrostatic dynamic equations, a thermodynamic equation, and a set of microphysics equations. The system was closed with Mellor-Yamada level 2.5 scheme [Mellor and Yamada, 1982] which explicitly solves for turbulent kinetic energy (TKE), while other second-order moments are parameterized. The coordinate system was rectangular Cartesian in the horizontal and terrain-following  $\sigma$ -type [Clark, 1977] in the vertical.

[14] For our simulations we used three nested grids centered on a complex patchy area around BR-364 (Figure 1). The coarsest grid, Grid 1, represented a  $800 \times 800$  km<sup>2</sup> domain with a horizontal grid spacing of 16 km; the second grid covered an area of  $312 \times 312$  km<sup>2</sup> with a grid spacing of 4 km; and in Grid 3, the finest grid, 1 km grid spacing was used to simulate an area of  $101 \times 101$  km<sup>2</sup>. For all three horizontal grids, the same stretched vertical grid was used with a 50 m grid spacing near the surface progressively increasing up to 1500 m aloft using a 1.15 stretch ratio. The model top reached a height of 24 km with 35 levels; the lowest 3 km was resolved with 18 grid elements to capture fine structures inside the PBL.

[15] The domain was initialized and nudged at the lateral and top boundaries of the coarsest grid with the National Centers for Environmental Prediction/National Center for Atmospheric Research (NCEP/NCAR) reanalysis data [Kalnay *et al.*, 1996]. For the outermost grid, the lower boundary conditions were derived from a soil-vegetation model based on the Avissar and Pielke [1989] parameterization scheme. The two inner grids were forced with observed fluxes of latent and sensible heat. It is important to emphasize that the purpose of this study is to evaluate whether or not mesoscale circulations develop in the tropical environment and how well such circulations can be simulated with RAMS. Therefore the focus is on the dynamics of the atmosphere. Imposing the fluxes, rather than simulating this boundary condition, eliminates a potential source of uncertainty associated with the soil-vegetation scheme and also saves computing time.

[16] These fluxes were measured during the Rondônia Boundary Layer Experiment phase 3 (RBLE-3) conducted during the Anglo-Brazilian Amazonian Climate Observation Study (ABRACOS) [Gash *et al.*, 1996]. They were measured every hour at two points, a forest site in Reserva Jaru (10°5'S, 61°55'W, 120 m (above mean sea level)) and a pasture site at Fazenda Nossa Senhora da Aparecida (10°45'S, 62°22'W, 220 m (above mean sea level)). The instruments used in both

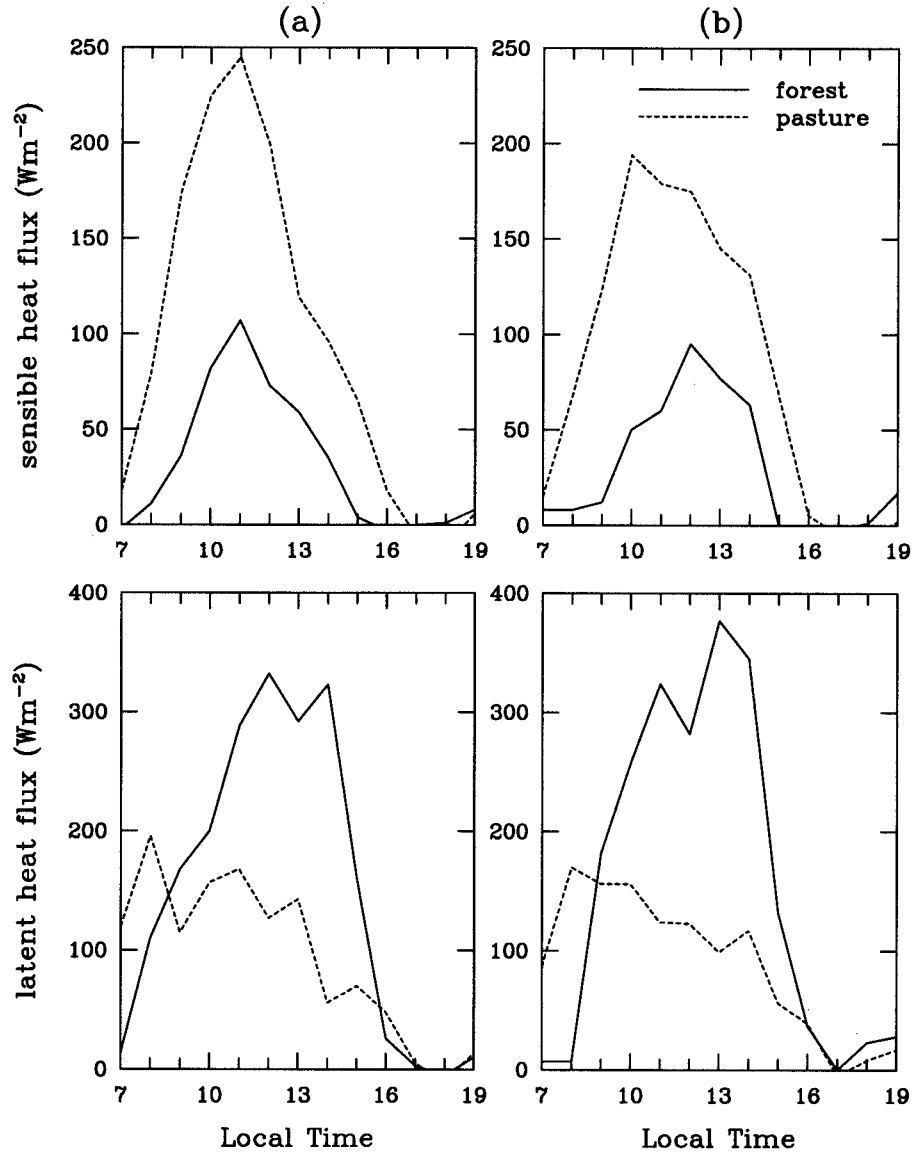


**Figure 2.** Surface fluxes of sensible heat (top) and latent heat (bottom) for (a) 17 August 1994 and (b) 22 August 1994.

towers have been discussed by *Shuttleworth et al.* [1988], and *McWilliam et al.* [1996] provide a detailed description of the sites. Complete flux data were available for only two days, 17 and 22 August 1994; and therefore only these two days were used for our study. The magnitude of the fluxes were typical wintertime (dry season) values in this region [*Fisch et al.*, 1996]. The maximum difference in sensible heat flux between the forest and the pasture site was more than  $100 \text{ Wm}^{-2}$ , while that of the latent heat flux was more than  $200 \text{ Wm}^{-2}$ , (Figure 2). In general, the sensible heat flux at the pasture site is much higher than that at the forest site, and vice versa for the latent heat flux. Given that evapotranspiration is expected to be higher in the forest, this is of course not surprising. This two-point observation was extrapolated to the entire domain based on the land-use pattern [*Calvet et al.*, 1997] with a random perturbation added to simulate turbulent departure. This representation is based on the reasonable presupposition

that ambient meteorology affecting the surface fluxes do not change much over a scale of 100 km. Errors introduced by this assumption were probably offset by the elimination of the uncertainties associated with the soil-vegetation scheme and its numerous unknown parameters.

[17] A *Chen and Cotton* [1983, 1987] type scheme was used for radiation. The finest grid explicitly resolves convection; no cumulus parameterization was used in the other grids since the scheme available in RAMS is applicable only for very coarse resolution grids.

[18] The simulations were run for 12 hours, 0700–1900 LT for both days. The output from Grid 3 is used for our analysis. The orography and land-use pattern in this grid is presented in Figure 3. The relatively wide band of pasture in the southwestern part of the domain is Highway BR-364; deforestation along this highway and the local roads make up the clearly evident fishbone pattern.

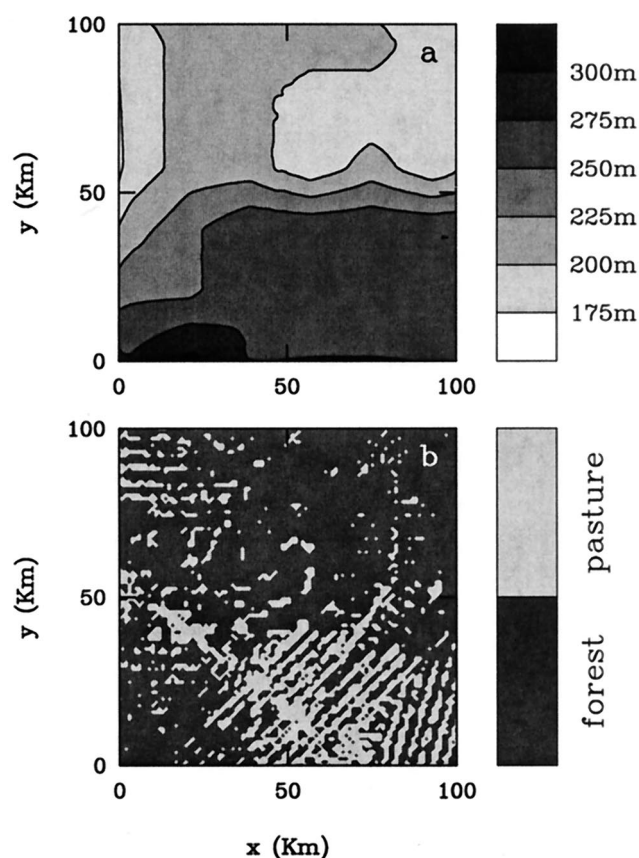


Figure 3. (a) Topography and (b) land-use pattern over Grid 3.

### 3. Results

#### 3.1. Impact of Surface Heterogeneity on Mesoscale Circulations

[19] To investigate how surface heterogeneity influences regional hydrometeorology, the simulation results for 17 Au-

gust were analyzed in detail. This was a day with moderate background synoptic flow, not more than a few meters per second near the surface, as evident from the wind profile shown in Figure 4. A horizontal cross-section of the simulated vertical velocity ( $w$ ) at a height of 493 m above ground level at successive times throughout the day shows the impact of the heterogeneous landscape on the dynamics of the atmosphere (Figure 5).

[20] In the morning, solar heating and vigorous mixing by turbulent thermals leads to the growth of the PBL. This can be seen in Figure 6 where the potential temperature profile (horizontally averaged over Grid 3) shows the development of a well-mixed layer by noon. Stronger sensible heating produces more intense turbulent eddies over the deforested areas in the morning, as shown in Figure 5. Hence the PBL over the pasture is higher than that over the forest by a few hundred meters, as indicated by the height of the inversion capping the convective boundary layer (CBL) in Figure 6. The PBL heights are well within the range observed by *Fisch et al.* [2000] during the course of RBLE-3 (for example  $1471 \pm 479$  m over pastures and  $902 \pm 307$  m over forests at 1400 LT). The mixed layer over the forest is shallower and hence denser than that over the pasture. These density gradients lead to horizontal pressure gradients between the forest and the pasture areas.

[21] In response to these pressure gradients, mesoscale circulations start to develop in the late morning. The eddies over Highway BR-364, aided by convergence from the surrounding forested regions, grow and coalesce to form the narrow updraft zone of the mesoscale circulations. The updraft velocity reaches a maximum of around  $0.4 \text{ ms}^{-1}$ . Thus the atmospheric dynamics over this region shifts from a turbulent regime in the morning to a mesoscale-dominated regime in the afternoon. Turbulence plays a very important role in setting up the pressure gradients required for the development of the mesoscale flow.

[22] The fact that the convergence starts over Highway

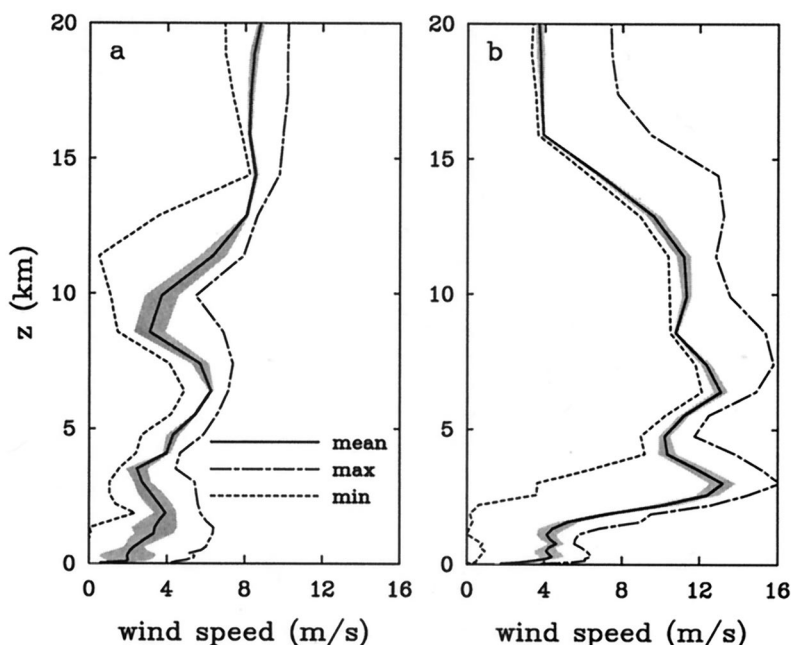


Figure 4. Vertical profile of horizontal wind speed averaged over grid 3 for the entire simulation period for (a) 17 August 1994 and (b) 22 August 1994; the shaded area represents a departure of one standard deviation from the mean.



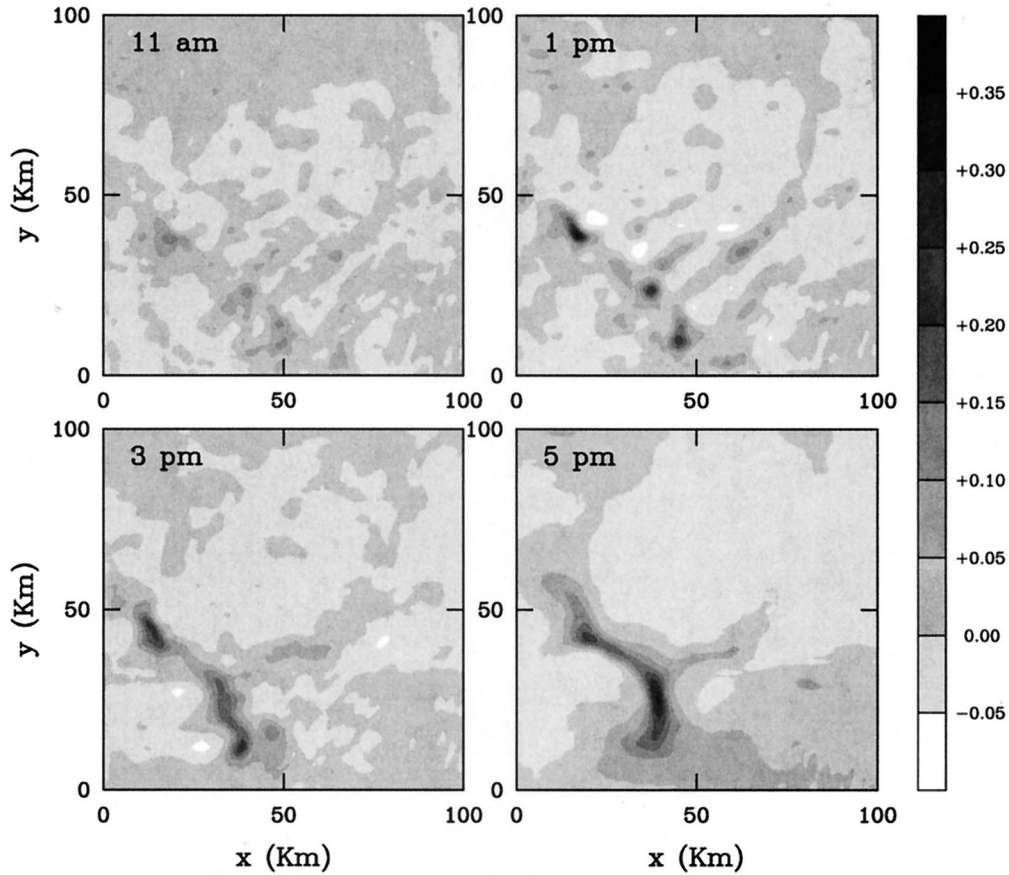


Figure 5. Evolution of vertical velocity ( $\text{ms}^{-1}$ ) at a height of 493 m for the REAL case on 17 August 1994.

BR-364 and not on smaller deforested patches indicates that a minimum length scale of heterogeneity is required to trigger organized circulations [Avisar and Schmidt, 1998; Gopalakrishnan et al., 2000; Baidya Roy and Avisar, 2000].

[23] Later in the day, a strong southwesterly synoptic wind advects the circulation northward. The position of the convergence zone is also slightly affected by a weak upslope flow that develops in late afternoon. Thus it appears that in this case the

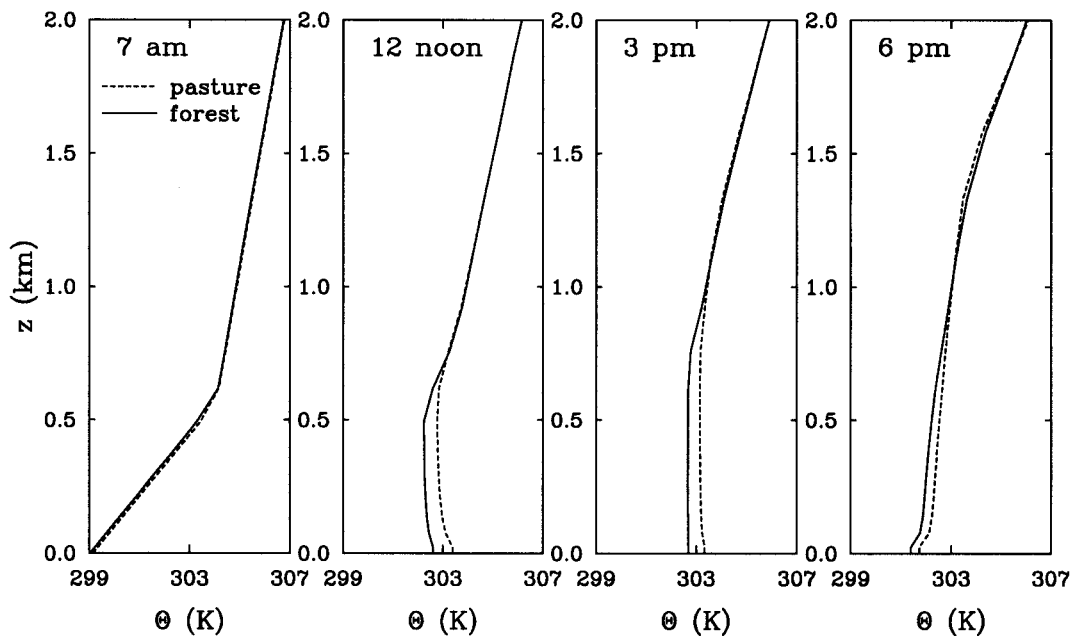


Figure 6. Vertical profiles of potential temperature at different times averaged separately over forest and pasture areas for the REAL case on 17 August 1994.

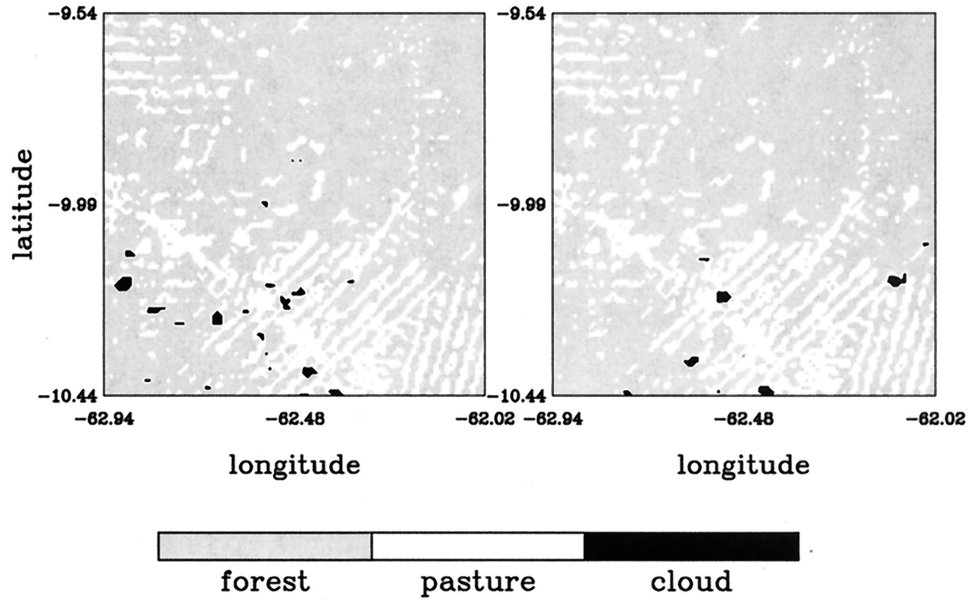


Figure 7. Land use pattern and clouds at 1500 LT on 17 August 1994 (left) and 22 August 1994 (right).

synoptic-scale winds merely reorient the coherent circulations and do not seem to significantly affect their strength as previously thought [Zhong and Doran, 1997; 1998].

[24] The model did not produce a significant amount of clouds or precipitation. The cause of this deficiency is a complex problem, probably related to the formulation of the cloud microphysical functions, which include a number of key variables whose values are not accurately known for the Amazonian environment. Another potential source of the problem is the lack of relevant information at initialization. To validate our results, we compare the location of the simulated updrafts with that of the clouds derived from Geostationary Earth Observing Satellite 7 (GOES 7) data. In the absence of other observational data, this can be a good way to evaluate the performance of the model in accurately simulating the dynamics of the mesoscale circulations. It can be seen that there is a strong correspondence between the  $w$  field and the shallow cumulus clouds that develop over the pasture along BR-364 (Figure 7). Details about how to identify clouds have been discussed in Appendix A. These clouds were shallow cumulus types with a very short lifespan ( $\sim 1$  hour) and the most common signature of surface-driven mesoscale circulations [Wang *et al.*, 2000]. The similarity between the flow fields and the clouds prove that RAMS does a good job in accurately simulating the atmospheric dynamics over this region.

[25] In addition to the simulation with real surface conditions, hereinafter referred to as the “REAL” case, the following experiments were conducted: (1) a “FOREST” case, where the two inner grids were assumed to be covered with forest and observed fluxes over the forest were imposed at the bottom boundary; (2) a “PASTURE” case, where the domain was assumed to be totally deforested and converted to pasture, and forced with surface fluxes observed at the pasture site; and (3) a “MEAN” case, where the domain was forced with a uniform flux obtained by averaging the forest and pasture fluxes weighted by their respective proportional areal coverage. Thus the total amount of sensible and latent heat entering the domain from the surface in this case is exactly equal to that for the REAL case. The results from these experiments were com-

pared with the REAL case to investigate the role of surface heterogeneity in producing coherent circulations and clouds.

[26] The results of the FOREST, PASTURE and MEAN runs (Figure 8) show weak upslope flows developing in response to the orography with the peak updraft velocities never exceeding a few centimeters per second. The PASTURE case produced slightly more intense circulations since the imposed surface sensible flux was higher than the other cases.

[27] The complete absence of coherent circulations in these simulations indicates that the mesoscale circulations simulated with the real landscape and the corresponding clouds observed by satellites can only be triggered by the surface heterogeneity.

### 3.2. Impact of Surface Heterogeneity on Vertical Fluxes

#### 3.2.1. Turbulent fluxes

[28] Grid 3, which covers a  $101 \times 101$  km<sup>2</sup> area, is equivalent in size to a single grid cell of a high resolution General Circulation Model (GCM). The potential for mesoscale circulations to affect synoptic-scale and global-scale processes can be estimated by studying their impact on vertical fluxes of heat and moisture spatially averaged over such a grid.

[29] The general shape of the turbulent flux profiles (Figure 9) for all cases is similar to that observed, simulated, and discussed in detail by many authors [Deardorff, 1974; Stull, 1988]. In the CBL, turbulence generated by buoyancy is strongly dependent on the surface fluxes and has a timescale of less than 1 hour. Hence the turbulent heat fluxes peak soon after the solar radiation maximum around midday and almost disappear after sundown.

[30] The turbulent sensible heat flux at 1300 LT shows a maximum at the surface associated with solar heating of the surface and decreases linearly upwards. Near the top of the mixed layer, the flux becomes negative due to entrainment of warmer air from the inversion layer capping the CBL. Since the surface sensible heat flux is higher in the pasture than in the forest, the turbulent sensible heat flux is the strongest in the PASTURE run and weakest in the FOREST run. The profiles for the REAL and MEAN cases are nearly identical,

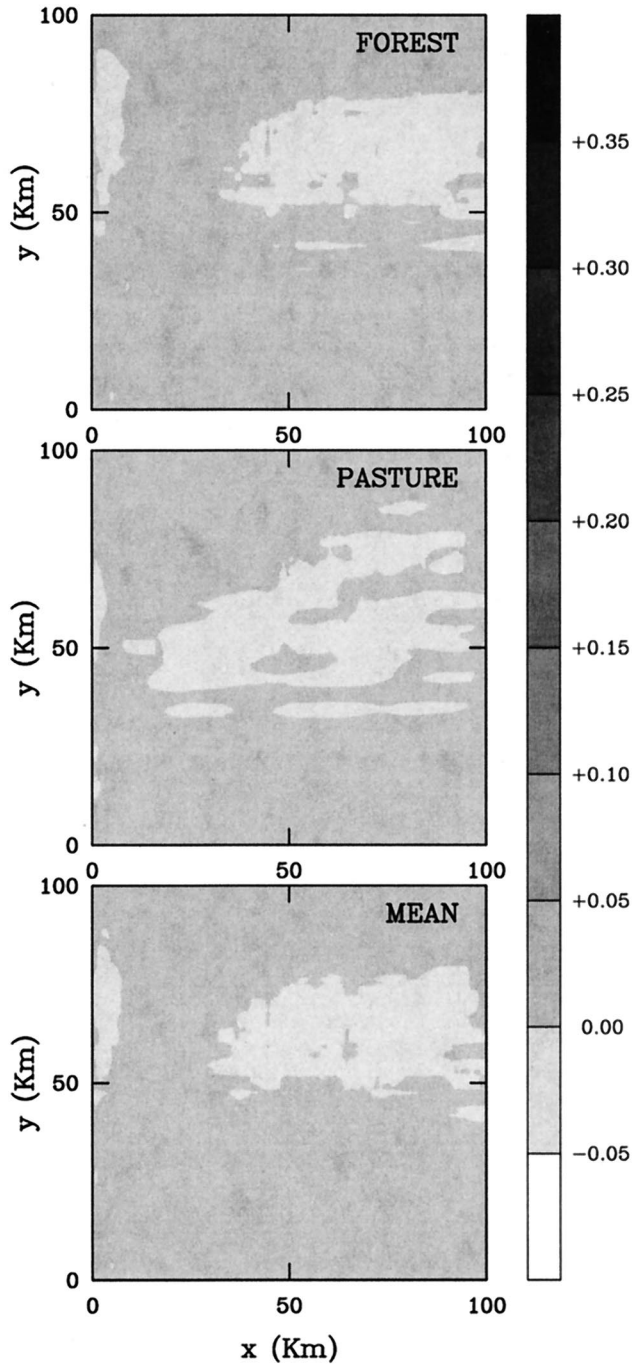


**Figure 8.** Vertical velocity ( $\text{ms}^{-1}$ ) at a height of 493 m at 1500 LT for FOREST, PASTURE, and MEAN runs using synoptic conditions for 17 August 1994.

indicating that the average turbulent flux of sensible heat is a very strong function of the mean surface sensible heat flux and is independent of surface heterogeneity.

[31] The turbulent latent heat flux is positive near the surface due to evaporation; it is also positive at the top of the mixed layer as a result of dry air being entrained from aloft. Evapotranspiration being much higher over the forest than over the pasture, the FOREST run produces the strongest turbulent latent heat flux and PASTURE the weakest. Though the mean surface evaporation rate is equal for the REAL and MEAN runs, the vertical profiles of the moisture flux are

considerably different. In the REAL case, as discussed later, mesoscale eddies enhance the mixing of moisture in the CBL, thereby reducing the vertical moisture gradient therein. Hence in this case, the turbulent latent heat flux is lower by up to  $100 \text{ Wm}^{-2}$  compared to that for the MEAN case. Thus surface heterogeneity and the resulting mesoscale circulations significantly affect turbulent transport of moisture in the PBL.

### 3.2.2. Mesoscale fluxes

[32] The signature of surface heterogeneity is readily apparent in the mesoscale fluxes (see *Avisar and Chen* [1993] for definition). As discussed earlier, turbulent eddies pave the way for the mesoscale rolls by setting up a horizontal pressure gradient. Hence the mesoscale fluxes start developing in late morning when turbulence is about to reach its maximum (Figure 10). The fluxes attain peak value in the early evening, implying a typical mesoscale timescale of a few hours.

[33] The vertical mesoscale sensible heat flux is positive in the lower part of the PBL, indicating upward transport of heat; near the top of the PBL, downward entrainment of warmer air results in a negative flux. Only the REAL case shows signs of pronounced mesoscale activity with flux values exceeding  $15 \text{ Wm}^{-2}$  at 1700 LT. The other cases show a small mesoscale flux associated with the orography-induced flow.

[34] The impact of this mesoscale flux can be best studied by comparing the domain-averaged vertical profile of potential temperature ( $\theta$ ) for the REAL and MEAN cases at 1800 LT. (Figure 11). At this time, turbulence being negligible for more than 1 hour,  $\theta$  is affected mostly by both mesoscale and synoptic scale processes for the REAL case and mostly by synoptic-scale processes in the MEAN case. These two cases have the same large-scale forcing and the same amount of thermal energy entering from the surface; hence the difference between the two profiles is due to the mesoscale processes arising from surface heterogeneity.

[35] In the absence of any source/sink or diffusion, the conservation equation for  $\bar{\theta}$  [Stull, 1988] is given by

$$\frac{d\bar{\theta}}{dt} = - \frac{\partial(\bar{u}_j \theta'_j)}{\partial x_j}. \quad (1)$$

Thus at any given level, the domain average  $\bar{\theta}$  is determined by the vertical gradient of the vertical flux at that level. It can be seen that up to 0.5 km from the surface, the vertical gradient of the flux is positive and the atmosphere is cooler in the REAL case. Between 0.5 and 1.3 km the flux decreases with height and a corresponding warming in the REAL case is obvious. Above this level, the atmosphere in the REAL case is slightly cooler than that in the MEAN run because the flux increases slowly with height. The overall implication of this is that the mesoscale circulations take heat from the lower part of the PBL and move it upward, thereby creating a much smoother profile of potential temperature. This vertical transport of heat results in cooler surface temperatures in the REAL case, even though the surface sensible heat flux is the same in both REAL and MEAN cases.

[36] The mesoscale transport of latent heat, similar to that of sensible heat, shows a strong response to the surface heterogeneity in the REAL simulation. The flux is negative (up to  $-50 \text{ Wm}^{-2}$ ) in the lower part of the PBL and positive (up to  $30 \text{ Wm}^{-2}$ ) aloft. The fluxes in the other cases show no sign of mesoscale activity except a weak signal associated with the orography-induced upslope flow discussed earlier.

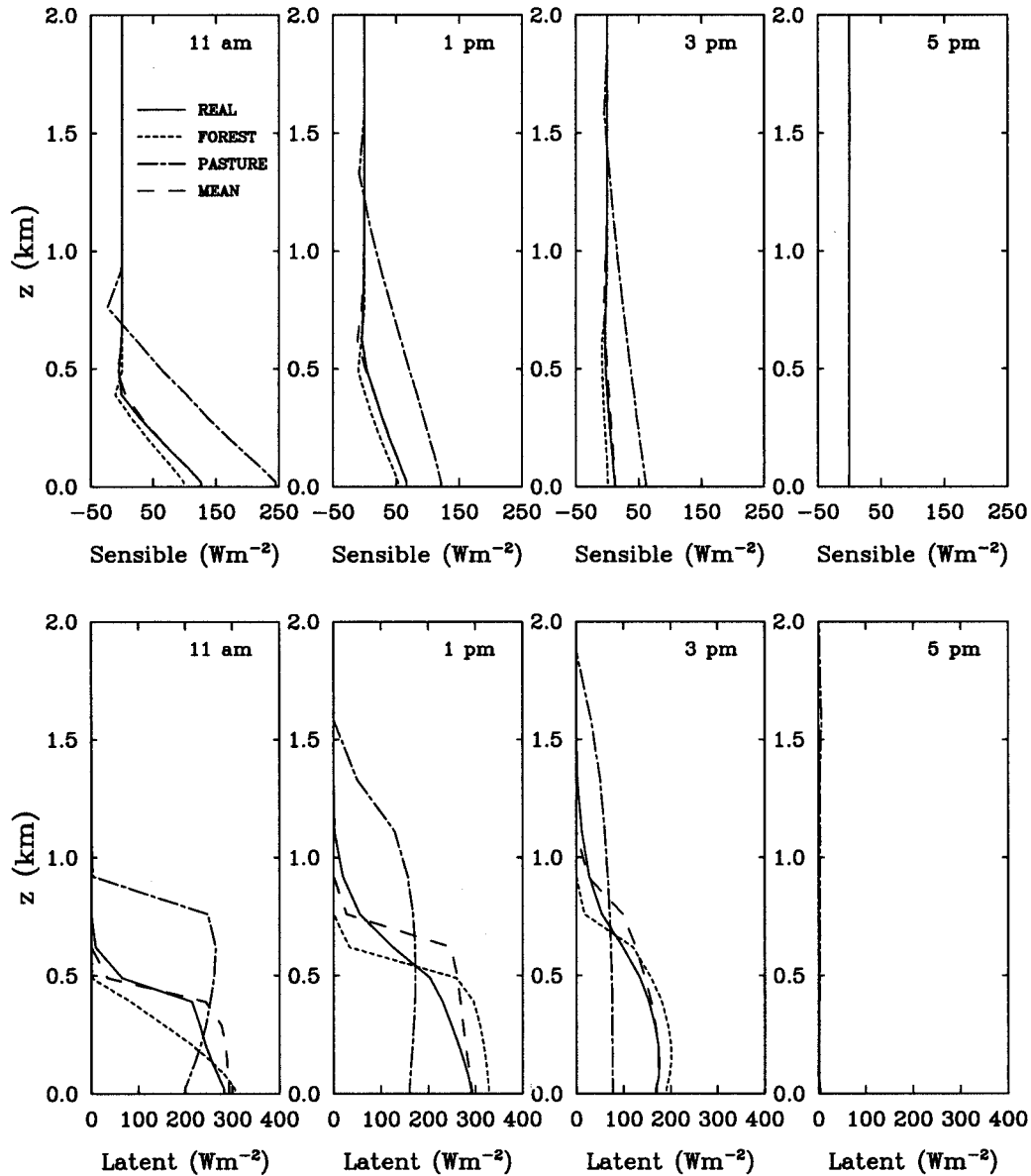


**Figure 9.** Horizontally averaged vertical turbulent flux of sensible heat and latent heat at different times for all cases on 17 August 1994.

[37] The pronounced impact of the mesoscale circulations on atmospheric moisture is evident in Figure 12, showing the horizontally averaged vertical profile of the water vapor mixing ratio at 1800 LT in the REAL and MEAN cases. Similar to  $\theta$ , the difference between the humidity profiles in the two cases is clearly dictated by the vertical gradient of the mesoscale latent heat flux. The atmosphere in the REAL case is wetter up to 0.5 km from the surface, drier between 0.5 and 1.2 km, and wetter aloft till the flux becomes zero around 2 km, while the flux gradients in those layers are negative, positive, and negative, respectively. The overall result is a smoother profile of specific humidity, almost linearly decreasing with height. The physical process that accomplishes this is complicated and seems to be intricately related to the nature of turbulence manifest earlier in the day. Turbulent eddies move moisture upward from the evaporating land surface, creating a temporary buildup aloft. This moisture is redistributed, both upward and downward, by the mesoscale circulations. Hence the mesoscale latent heat

flux is positive above and negative below the layer with excess moisture. This vertical transport of moisture results in higher surface humidity in the REAL case, even though the surface latent heat flux is the same in both REAL and MEAN cases.

[38] In the morning, upward transport of moisture by turbulent eddies masks the downward component of the mesoscale latent heat flux. The downward component becomes prominent only in the afternoon when turbulence has subsided.

[39] The transport of heat and moisture by mesoscale eddies significantly alters the mean state of the atmosphere. For example, calculations show that at a height of 1.2 km from the surface, the atmosphere in the REAL case is 4% higher in relative humidity and cooler by 0.2 K. This can be a deciding factor in condensation and formation of clouds that can change the thermal and radiative state of the atmosphere through complex feedbacks. August being wintertime in Rondônia, the surface fluxes are relatively weak. The summertime values are



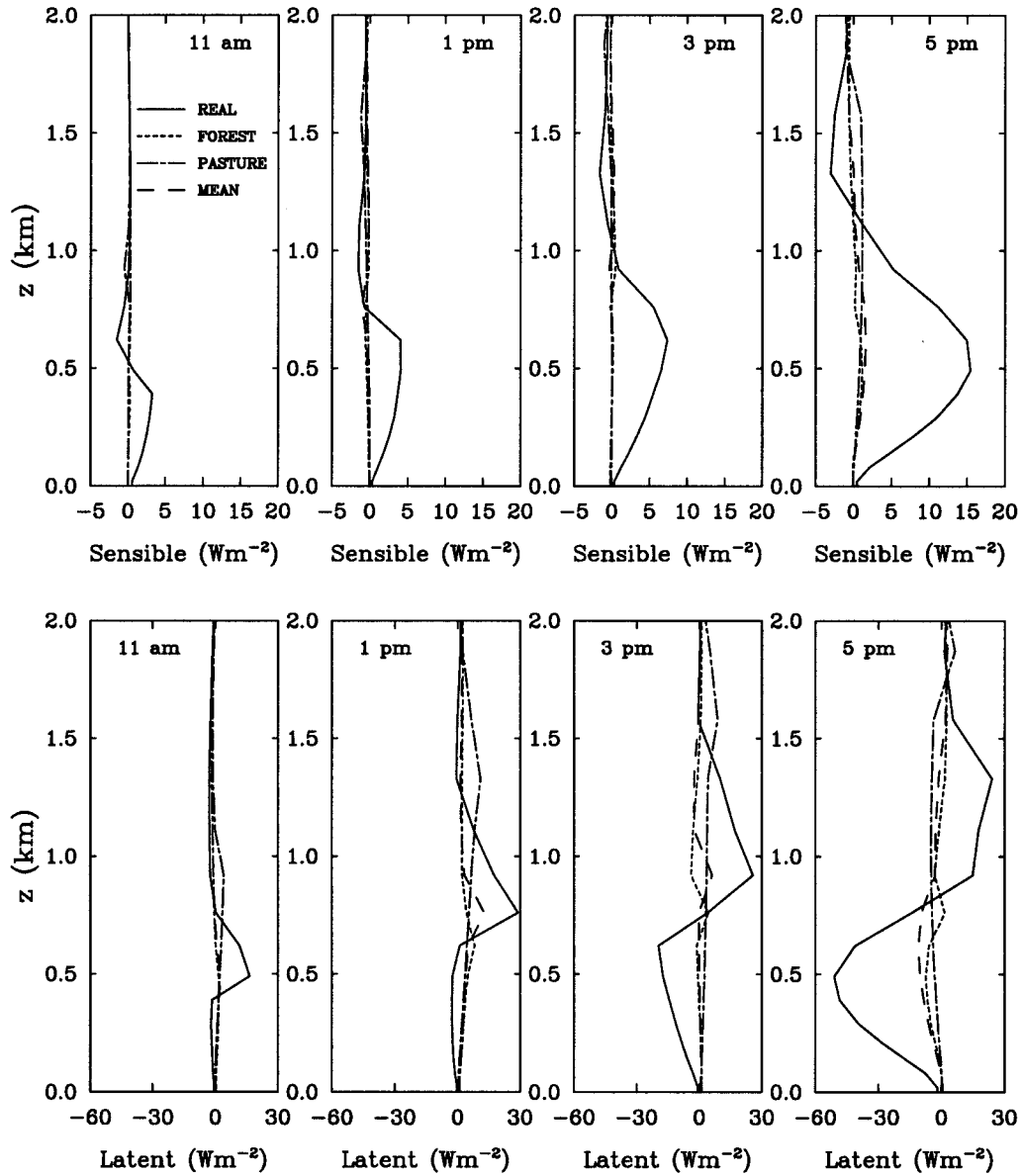


Figure 10. Same as Figure 9 but for mesoscale flux.

much larger and the potential impact of that could be much stronger.

[40] The peak values of horizontally averaged mesoscale fluxes are smaller than that of turbulent fluxes. However, one needs to keep in mind that mesoscale circulations are localized, while turbulence is active in the entire domain. Locally, the mesoscale fluxes are quite intense; near the mesoscale updraft zones, the fluxes are 1 order of magnitude higher than their domain-averaged value. Additionally, mesoscale and turbulent processes have different length and time scales. Turbulence is more important near the ground, while mesoscale processes are stronger aloft; for example, the positive mesoscale flux of moisture in the upper PBL is always greater than the turbulent flux at that height. Also, while turbulent transport is stronger in the morning, later in the day, most of the transport of heat and moisture in the PBL is carried out by mesoscale eddies. Thus the contribution of mesoscale eddies in

PBL dynamics cannot be evaluated by simply comparing the peak values of mesoscale and turbulent fluxes.

### 3.3. Impact of Synoptic-Scale Flow on the Mesoscale Circulations

[41] The background meteorological conditions on our second case study day (22 August 1994) were quite different from the previous case. On this day, a strong westerly low-level jet with mean wind speed more than  $12 \text{ ms}^{-1}$ , and gusting to  $16 \text{ ms}^{-1}$ , was blowing throughout the day (Figure 4). In spite of the strong wind, convergence developed over the road around noon, but by early afternoon, the convergence zone was advected eastward (Figure 13). In early evening, all that was left was a few localized, intense updrafts in the southeastern part of the domain. Scattered shallow clouds observed in that region (Figure 7) indicate that the model was successfully simulating the atmospheric dynamics.

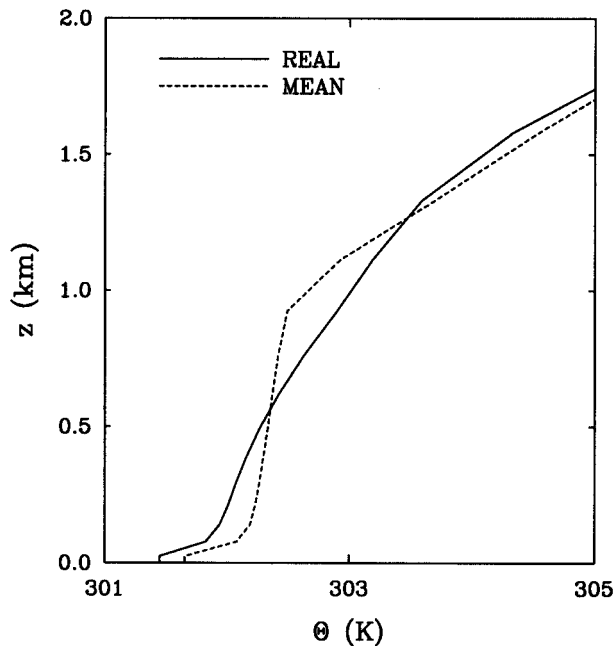


**Figure 11.** Horizontally averaged vertical profile of potential temperature for the REAL and MEAN cases at 1800 LT on 17 August 1994.

[42] The PBL developed in this case was shallower than that on 17 August by a few hundred meters, but in spite of the strong large-scale wind, the patterns and the magnitudes of mesoscale heat and moisture fluxes were very similar in both cases. No evidence of coherent circulations were observed when homogeneous conditions were imposed at the bottom boundary.

[43] Thus contrary to the conclusions of *Dalu et al.* [1996], *Wang et al.* [1996], and *Zhong and Doran* [1997, 1998], this

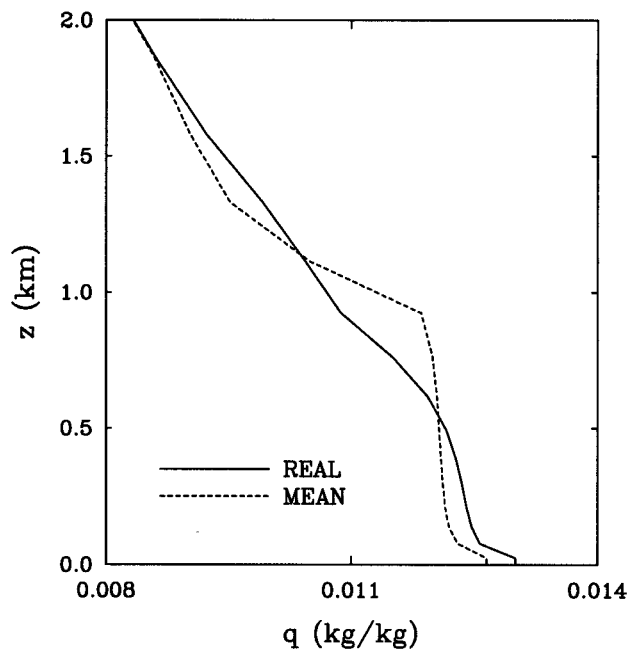


**Figure 12.** Same as Figure 11 but for water vapor mixing ratio.

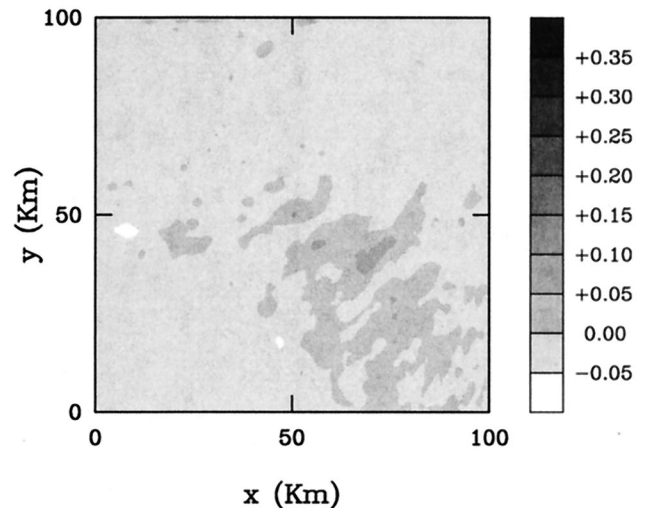


**Figure 13.** Vertical velocity ( $\text{ms}^{-1}$ ) at a height of 493 m at 1500 LT for the REAL case on 22 August 1994.

study proves that coherent surface-driven mesoscale circulations and corresponding mesoscale fluxes can develop in spite of strong synoptic winds.

#### 4. Conclusions

[44] A high-resolution mesoscale model was used to simulate the atmosphere above a deforested part of Amazonia. Earlier modeling studies have been criticized for their simplicity in representing surface heterogeneity and for neglecting the impact of ambient meteorology. Indeed, a few test cases over the same domain, run with no large-scale gradients, produced very strong updrafts. When the effect of synoptic-scale conditions was included, the circulations became weaker but did not disappear. Surface heterogeneity triggered the mesoscale circulations; they were then advected by the large-scale flow. The signature of these circulations was clearly evident in satellite-derived cloud images. No such circulation developed when homogeneous conditions were imposed at the surface.

[45] Realistic background conditions were assumed by forcing the boundaries of the domain with observed fluxes and meteorological data. Coherent circulations evolved even with very strong low-level jets. This indicates that mesoscale circulations can be produced under a much wider range of large-scale conditions than previously thought.

[46] Due to a lack of forcing data, only a limited number of case studies with different synoptic flow regimes were used for our numerical experiments. Though they have vastly different characteristics, obviously, this is not an exhaustive representation of the whole gamut of synoptic-scale conditions that can be found over Amazonia in the dry season. Hence more case studies need to be performed with different background conditions. Additionally, we intend to use the data collected as a part of the Large-Scale Biosphere-Atmosphere wet season Atmospheric Measurement Campaign (WETAMC/LBA) in January–February 1999, in Rondônia, to conduct similar experiments exploring the possibilities of the evolution of surface-driven coherent circulations in the rainy season as well.

[47] A major problem with these circulations is that they cannot be observed with conventional meteorological networks. Occasionally, they are masked by strong synoptic and

orography-induced wind and can be seen only as a perturbation from the mean flow. The clouds often produced by these circulations are small, shallow cumulus type with a very short life span and difficult to observe in satellite images. Also, since the circulations can be advected by large-scale winds, the clouds are not always anchored to the surface heterogeneity pattern; hence the circulations are not readily apparent. Thus, dedicated field experiments are required to observe these mesoscale processes. The results of this study can be used to design experiments geared toward observing mesoscale circulations during the upcoming LBA dry season campaign scheduled for 2002.

[48] These circulations strongly influence the transport of heat and moisture at the GCM scale. The sensible heat flux is small, but the mesoscale latent heat flux is at least as large as the turbulent flux in the upper PBL. These processes are subgrid scale for a typical GCM. However, the subgrid parameterizations for current GCMs are based mostly on turbulence; no mesoscale processes except gravity waves are considered. Adequate parameterizations for these processes should be included in GCMs for a better simulation of climate. As evident from this study, both stationary parameters, like scale of surface heterogeneity, as well as nonstationary parameters, like ambient meteorology, play important roles in the evolution of these circulations. This should be taken into account while developing a physically based parameterization for these processes.

[49] Any parameterization for GCMs should be applicable for the entire globe. Weaver and Avissar [2001] have used GCIP data to investigate mesoscale circulations in the midlatitudes in North America. Additional insights have also been provided by Vidale *et al.* [1997] using BOREAS data at high latitudes. Similar studies need to be carried out with different kinds of surface heterogeneity and synoptic-scale forcing over other climatic regions using data from relevant field experiments. This study over tropical Amazonia can be used in conjunction with others to develop a comprehensive and universal parameterization for this phenomenon.

## Appendix A: Cloud Identification

[50] Hourly data from the seventh Geostationary Operational Environmental Satellite (GOES 7) were used to identify clouds developing over the domain. Brightness ( $B_{\text{vis}}$  from the visible channel (centered at  $0.65 \mu$ , 1 km resolution) was converted to albedo ( $\alpha$ ) using the formula

$$\alpha = (aB_{\text{vis}}^2 + b)/(I_0 \cos \zeta), \quad (\text{A1})$$

where  $a$ ,  $b$ , and  $I_0$  are calibration parameters for the GOES-7 sensor equaling  $0.00539 \text{ Wm}^{-2}$ ,  $-2.67 \text{ Wm}^{-2}$ , and  $336 \text{ Wm}^{-2}$ , respectively;  $\zeta$  is the solar zenith angle. Temperature ( $T$ ) can be obtained from infrared brightness ( $B_{\text{IR}}$ ) from channel 8 (centered around  $11.2 \mu$ , originally 4 km resolution, interpolated to a 1 km grid using kriging technique) from the relation

$$\begin{aligned} T &= 418 - B_{\text{IR}}, & (B_{\text{IR}} \geq 176), \\ T &= 330 - B_{\text{IR}}/2, & (B_{\text{IR}} \leq 176). \end{aligned} \quad (\text{A2})$$

[51] Clouds typically have an albedo of 0.3 or more [Hartmann, 1994]; in contrast, the forest and pasture areas in Rondônia have albedoes of 0.12 and 0.15, respectively, in the dry season [Silva Dias and Regnier, 1996]. Also, from our simula-

tions and observations the average temperature near the top of the PBL was found to be 293 K.

[52] These two parameters were used to identify clouds as bright spots with albedo greater than 0.3 and temperature less than 293 K. This dual filtering method is very simplistic and does not distinguish between high and low clouds; due to the strict albedo requirement, it probably underestimates the cloudiness as well. However, this algorithm can pinpoint the location of day-time clouds with a very high degree of accuracy.

[53] **Acknowledgments.** The authors would like to thank D. W. Martin and A. Negri for helping with the satellite data and M. A. F. de Silva Dias and P. L. de Silva Dias for their insights.

## References

- Avissar, R., and F. Chen, Development and analysis of prognostic equations for mesoscale kinetic energy and mesoscale (subgrid scale) fluxes for large-scale atmospheric models, *J. Atmos. Sci.*, **50**, 3751–3774, 1993.
- Avissar, R., and Y. Liu, Three-dimensional numerical study of shallow convective clouds and precipitation induced by land-surface forcing, *J. Geophys. Res.*, **101**, 7499–7518, 1996.
- Avissar, R., and R. A. Pielke, A parameterization of heterogeneous land surfaces for atmospheric numerical models and its impact on regional meteorology, *Mon. Weather Rev.*, **117**, 2113–2136, 1989.
- Avissar, R., and T. Schmidt, An evaluation of the scale at which ground-surface heat flux patchiness affects the convective boundary layer using large-eddy simulations, *J. Atmos. Sci.*, **55**, 2666–2689, 1998.
- Baidya Roy, S., and R. Avissar, Scales of response of the convective boundary layer to surface heterogeneity, *Geophys. Res. Lett.*, **27**, 533–536, 2000.
- Calvet, J. C., R. Santos-Alvalá, G. Jaubert, C. Delire, C. Nobre, I. Wright, and J. Noilhan, Mapping surface parameters for mesoscale modeling in forested and deforested south-western Amazonia, *Bull. Am. Meteorol. Soc.*, **78**, 413–423, 1997.
- Chen, C., and W. R. Cotton, A one-dimensional simulation of the stratocumulus-capped mixed layer, *Boundary Layer Meteorol.*, **25**, 289–321, 1983.
- Chen, C., and W. R. Cotton, The physics of the marine stratocumulus-capped mixed layer, *J. Atmos. Sci.*, **44**, 2951–2977, 1987.
- Chen, F., and R. Avissar, The impact of land-surface wetness heterogeneity on mesoscale heat fluxes, *J. Appl. Meteorol.*, **33**, 1323–1340, 1994a.
- Chen, F., and R. Avissar, Impact of land-surface moisture variability on local shallow convective cumulus and precipitation in large-scale models, *J. Appl. Meteorol.*, **33**, 1382–1401, 1994b.
- Clark, T. L., A small-scale dynamic model using a terrain following coordinate transformation, *J. Comput. Phys.*, **24**, 186–215, 1977.
- Copeland, J. H., R. A. Pielke, and T. G. F. Kittel, Potential climatic impacts of vegetation change: A regional modeling study, *J. Geophys. Res.*, **101**, 7409–7418, 1996.
- Cutrim, E., D. W. Martin, and R. Rabin, Enhancement of cumulus clouds over deforested lands in Amazonia, *Bull. Am. Meteorol. Soc.*, **76**, 1801–1805, 1995.
- Dalu, G. A., and R. A. Pielke, Vertical heat fluxes generated by mesoscale atmospheric flow induced by thermal inhomogeneities in the PBL, *J. Atmos. Sci.*, **50**, 919–926, 1993.
- Dalu, G. A., R. A. Pielke, M. Baldi, and X. Zheng, Heat and momentum fluxes induced by thermal inhomogeneities, *J. Atmos. Sci.*, **53**, 3286–3302, 1996.
- Deardorff, J. W., Three-dimensional numerical study of the height and mean structure of a heated planetary boundary layer, *Boundary Layer Meteorol.*, **7**, 81–106, 1974.
- Dolman, A. J., M. A. F. Silva Dias, J. C. Calvet, M. Ashby, A. S. Tahara, C. Delire, P. Kabat, G. A. Fisch, and C. A. Nobre, Mesoscale effects of tropical deforestation in Amazonia: Preparatory modeling studies, *Ann. Geophys.*, **17**, 1095–1110, 1999.
- Doran, J. C., W. J. Shaw, and J. M. Hubbe, Boundary layer characteristics over areas of inhomogeneous surface fluxes, *J. Appl. Meteorol.*, **34**, 559–571, 1995.

- Fearnside, P. M., Deforestation in Brazilian Amazonia: The effect of population and land tenure, *Ambio*, 22, 537–545, 1993.
- Fisch, G., A. D. Culf, and C. A. Nobre, Modeling convective boundary layer growth in Rondônia, in *Amazonian Deforestation and Climate*, edited by J. H. C. Gash, C. A. Nobre, J. M. Roberts and R. L. Victoria, pp. 425–435, John Wiley, New York, 1996.
- Fisch, G., J. Tota, L. Machado, B. Ferrier, M. A. F. Silva Dias, A. J. Dolman, J. Halverson, and J. D. Fuentes, Atmospheric boundary layer growth during LBA/TRMM experiment, in *Preprints of 15th Conference on Hydrology*, pp. 319–322, Am. Meteorol. Soc., Boston, Mass, 2000.
- Gash, J. H. C., and C. A. Nobre, Climatic effects of Amazonian deforestation: Some results from ABRACOS, *Bull. Am. Meteorol. Soc.*, 78, 823–830, 1997.
- Gash, J. H. C., C. A. Nobre, J. M. Roberts, and R. L. Victoria, An overview of ABRACOS, in *Amazonian Deforestation and Climate*, edited by J. H. C. Gash, C. A. Nobre, J. M. Roberts, and R. L. Victoria, pp. 1–14, John Wiley, New York, 1996.
- Gopalakrishnan, S. G., S. Baidya Roy, and R. Avissar, An evaluation of the scale at which topographical features affect the convective boundary layer using large-eddy simulations, *J. Atmos. Sci.*, 57, 334–351, 2000.
- Hartmann, D. L., *Global Physical Climatology*, 411 pp, Academic, San Diego, Calif, 1994.
- Kalnay, E. et al., The NCEP/NCAR 40-year reanalysis project, *Bull. Am. Meteorol. Soc.*, 77, 437–471, 1996.
- Li, B., and R. Avissar, The impact of spatial variability of land surface heat fluxes, *J. Clim.*, 7, 527–537, 1994.
- Liston, G. E., and R. A. Pielke, A climate version of the regional atmospheric modeling system, *Theor. Appl. Climatol.*, 66, 29–47, 2000.
- Lynn, B., D. Rind, and R. Avissar, The importance of mesoscale circulations generated by subgrid-scale landscape heterogeneities in general circulation models, *J. Clim.*, 8, 191–205, 1995.
- Mahrt, L., J. Sun, D. Vickers, J. I. MacPherson, J. R. Pederson, and R. Desjardins, Observations of fluxes and inland breezes over a heterogeneous surface, *J. Atmos. Sci.*, 51, 2484–2499, 1994.
- McWilliam, A. L. C., O. M. R. Cabral, B. M. Gomes, J. L. Estevez, and J. M. Roberts, Forest and pasture leaf-gas exchange in southwest Amazonia, in *Amazonian Deforestation and Climate*, edited by J. H. C. Gash, C. A. Nobre, J. M. Roberts, and R. L. Victoria, pp. 413–424, John Wiley, New York, 1996.
- Mellor, G. L., and T. Yamada, Development of a turbulence closure model for geophysical fluid problems, *Rev. Geophys.*, 20, 851–875, 1982.
- Physick, W. L., and N. J. Tapper, Numerical study of circulations induced by dry salt lake, *Mon. Weather Rev.*, 118, 1029–1042, 1990.
- Pielke, R. A., W. R. Cotton, R. L. Walko, C. J. Tremback, M. E. Nicholls, M. D. Moran, D. A. Wesley, T. J. Lee, and J. H. Copeland, A comprehensive meteorological modeling system-RAMS, *Meteorol. Atmos. Phys.*, 49, 69–91, 1992.
- Pielke, R. A., R. Avissar, M. Raupach, A. J. Dolman, X. Zeng, and A. S. Denning, Interactions between the atmosphere and terrestrial ecosystems: Influence on weather and climate, *Global Change Biol.*, 4, 461–475, 1998.
- Rabin, R. M., and D. W. Martin, Satellite observations of shallow cumulus coverage over the central United States: An exploration of land use impact on cloud cover, *J. Geophys. Res.*, 101, 7149–7155, 1996.
- Rabin, R. M., S. Stadler, P. J. Wetzel, D. J. Stensrud, and M. Gregory, Observed effects of landscape variability on convective clouds, *Bull. Am. Meteorol. Soc.*, 71, 272–280, 1990.
- Segal, M., and R. W. Arritt, Nonclassical mesoscale circulations caused by surface sensible heat-flux gradients, *Bull. Am. Meteorol. Soc.*, 73, 1593–1604, 1992.
- Segal, M., W. E. Schreiber, G. Kallos, J. R. Garratt, A. Rodi, J. Weaver, and R. A. Pielke, The impact of crop areas in northeast Colorado on midsummer mesoscale thermal circulations, *Mon. Weather Rev.*, 117, 809–825, 1989.
- Segal, M., J. H. Cramer, R. A. Pielke, J. R. Garratt, and P. Hildebrand, Observational evaluation of the snow breeze, *Mon. Weather Rev.*, 119, 412–424, 1991.
- Seth, A., and F. Giorgi, Three-dimensional model study of organized mesoscale circulations induced by vegetation, *J. Geophys. Res.*, 101, 7371–7391, 1996.
- Shuttleworth, W. J., J. H. C. Gash, C. R. Lloyd, D. D. McNeil, C. J. Moore, and J. S. Wallace, An integrated micrometeorological system for evaporation measurements, *Agric. For. Meteorol.*, 43, 295–317, 1988.
- Silva Dias, M. A. F., and P. Regnier, Simulation of mesoscale circulations in a deforested area of Rondônia in the dry season, in *Amazonian Deforestation and Climate*, edited by J. H. C. Gash, C. A. Nobre, J. M. Roberts and R. L. Victoria, pp. 531–547, John Wiley, New York, 1996.
- Skole, D., and C. Tucker, Tropical deforestation and habitat fragmentation in the Amazon: Satellite data from 1978 to 1988, *Science*, 260, 1905–1910, 1993.
- Skole, D., W. H. Chomentowski, W. A. Salas, and A. D. Nobre, Physical and human dimensions of deforestation in Amazonia, *Bio-science*, 44, 314–322, 1994.
- Stull, R. B., *An Introduction to Boundary Layer Meteorology*, 666 pp., Kluwer Acad., Norwell, Mass, 1988.
- Vidale, P. L., R. A. Pielke, L. T. Steyaert, and A. Barr, Case study modeling of turbulent and mesoscale fluxes over the BOREAS region, *J. Geophys. Res.*, 102, 29,167–29,188, 1997.
- Wang, J., R. Bras, and E. A. B. Eltahir, A stochastic linear theory of mesoscale circulation induced by the thermal heterogeneity of the land surface, *J. Atmos. Sci.*, 53, 3349–3366, 1996.
- Wang, J., R. Bras, and E. A. B. Eltahir, Numerical simulation of nonlinear mesoscale circulations induced by the thermal heterogeneities of land surface, *J. Atmos. Sci.*, 55, 447–464, 1998.
- Wang, J., R. Bras, and E. A. B. Eltahir, The impact of observed deforestation on the mesoscale distribution of rainfall and clouds in Amazonia, *J. Hydrometeorol.*, 1, 267–286, 2000.
- Weaver, C. P. and R. Avissar, Atmospheric disturbances caused by human modification of the landscape, *Bull. Am. Meteorol. Soc.*, 82, 269–281, 2001.
- Wetzel, P. J., S. Argenti, and A. Boone, Role of land surface in controlling daytime cloud amount: Two case studies in the GCIP-SW area, *J. Geophys. Res.*, 101, 7359–7370, 1996.
- Zhong, S., and J. C. Doran, A study of the effects of spatially varying fluxes on cloud formation and boundary layer properties using data from the southern Great Plains cloud and radiation testbed, *J. Clim.*, 10, 327–341, 1997.
- Zhong, S., and J. C. Doran, An evaluation of the importance of surface flux variability on GCM-scale boundary-layer characteristics using realistic meteorological and surface forcing, *J. Clim.*, 11, 2774–2788, 1998.

R. Avissar, Department of Civil and Environmental Engineering, Edmund T. Pratt Jr. School of Engineering, Duke University, 123 Hudson Hall, Durham, NC 27708-0287, USA. (avissar@duke.edu)

S. Baidya Roy, Department of Ecology and Evolutionary Biology/Princeton Environmental Institute, Princeton University, Princeton, NJ 08544-1003, USA. (sroy@princeton.edu)